STEP inhibition prevents Aβ-mediated damage in dendritic complexity and spine density in Alzheimer's disease.

Manavi Chatterjee[1*], Jeemin Kwon[1], Jessie Benedict[1], Marija Kamceva[1], Pradeep Kurup[1] and Paul J. Lombroso[1,2,3*]

[1]Child Study Center and Departments of [2]Psychiatry, and [3]Neurobiology, Yale University, 230 South Frontage Rd, New Haven, CT, 06520.

Corresponding authors

***Manavi Chatterjee: manavi.chatterjee@yale.edu, phone (203) 785-5235**

*** Paul Lombroso: paul.lombroso@yale.edu, phone (203) 737-2224**

Abstract

Loss of dendritic spines and decline of cognitive function are hallmarks of patients with Alzheimer's disease (AD). Previous studies have shown that AD pathophysiology involves increased expression of a central nervous system-enriched protein tyrosine phosphatase called STEP (STriatal-Enriched protein tyrosine Phosphatase). STEP opposes the development of synaptic strengthening by dephosphorylating substrates, including GluN2B, Pyk2 and ERK1/2. Genetic reduction of STEP as well as pharmacological inhibition of STEP improves cognitive function and hippocampal memory in the 3xTg AD mouse model. Here, we show that the improved cognitive function is accompanied by an increase in synaptic connectivity in cell cultures as well as in the triple transgenic AD mouse model, further highlighting the potential of STEP inhibitors as a therapeutic agent.

Keywords:

STEP, TC-2153, dendritic complexity, spine density, Alzheimer's disease

Abbreviations

STEP = STriatal-Enriched protein tyrosine Phosphatase

AD = Alzheimer's disease

3xTg = triple transgenic mouse model

CM = conditioned medium

CNS = central nervous system

ANOVA = analysis of variance

Aβ = beta amyloid

GluN2B = glutamate ionotropic receptor NMDA type subunit 2B

GluA2 = glutamate ionotropic receptor AMPA type subunit 2

Pyk2 = protein tyrosine kinase 2

ERK1/2 = extracellular signal-regulated kinase-1

SPIN90 = SH3 protein interacting with Nck, 90 kDa

WT = wild-type

1. Introduction

Alzheimer's disease (AD) is the most common form of dementia and leads to a progressive disruption of cognitive function. Age-dependent synapse loss and concomitant memory impairment is common in patients with Alzheimer's (Terry et al. 1991) as well as many transgenic mouse models of AD, including the triplet transgeneic (3xTg) AD mouse model (Knobloch and Mansuy 2008). Notably, in patients with early-stage AD, dendritic spine density is reduced in the frontal cortex and hippocampal CA1 region (DeKosky and Scheff 1990; Scheff et al. 2006). The loss of spines caused by beta-amyloid (Aβ) peptide during the prodromal phase of AD has been reported to precede disintegration of neuronal networks and consequent cognitive decline (Palop and Mucke 2010; Kashyap et al. 2019). Hence, investigation of targets that could reduce spine loss is of paramount importance in understanding disease progression as well as for translational interventions.

STriatal-Enriched protein tyrosine Phosphatase (STEP) is one such target affected by Aβ accumulation in the brain. STEP is a CNS enriched phosphatase that opposes synaptic strengthening by dephosphorylating key synaptic kinases, including ERK1/2, Fyn, and Pyk2, leading to their inactivation (Venkitaramani et al. 2009; Xu et al. 2012; Li et al. 2014). STEP also dephosphorylates the GluN2B and GluA2 subunits of NMDA and AMPA receptors, leading to the internalization of these receptor complexes (Snyder et al. 2005; Zhang et al. 2008; Wu et al. 2011).

STEP is implicated in several neuropsychiatric disorders, including Alzheimer's disease (Kurup et al. 2010; Zhang et al. 2010), Parkinson's disease (Kurup et al. 2015), schizophrenia (Xu et al. 2018), fragile X syndrome (Chatterjee et al. 2018), as well as age-related memory decline (Castonguay et al. 2018). In AD, STEP levels are elevated in post-mortem human patients and also in several AD mouse models: Tg2576 (Kurup et al. 2010), J20 (Chin et al. 2005), APP/PS1 (Zhang et al. 2013) and 3xTG mice (Zhang et al. 2010). The accumulation of beta-amyloid (Aβ) in AD leads to the blockade of the ubiquitin-proteosome system (UPS) and activation of α7 nicotinic receptors, both processes that eventually lead to increased levels of activated STEP (Kurup et al. 2010; Zhang et al. 2013). In 3xTg-AD mice, STEP activity is significantly elevated after six months of age, which coincides with the start of memory deficits (Zhang et al. 2010).

Genetic reduction of STEP reversed the cognitive deficits experienced by 6-12 month-old 3xTg AD mouse models, thus validating STEP as a target for drug discovery (Zhang et al. 2010). The discovery and administration of a potent and specific STEP inhibitor, 8-(trifluoromethyl)-1,2,3,4,5-benzopentathiepin-6-amine hydrochloride (TC-2153), to 6-month-old 3xTg AD mice reversed the cognitive deficits in these mice (Xu et al. 2014).

As recent studies point to the involvement of STEP in spine dynamics (Cho et al. 2013b; Ng et al. 2014), we tested the hypothesis that inhibition of STEP would rescue the loss of spines in neuronal cultures and in 6-month-old 3xTg mice.

2. Experimental Procedures

2.1 Animals: All protocols were approved by the Yale University Institutional Animal Care and Use Committee and strictly adhered to the NIH Guide for the Care and Use of Laboratory Animals. C57Bl/6 and 3xTg mice on C57BL/6/SV129 background were used for the experiments. Animals were housed in groups of 2–5 in standard vented-rack cages in a 12:12 h light:dark cycle with food and water available ad libitum.

2.2 7PA2-conditioned medium preparation. 7PA2 cells-conditioned medium (7PA2-CM; Aβ-enriched) was prepared as described previously with minor modifications (Walsh et al. 2002). The 7PA2 cells excrete Aβ oligomers, primarily dimers and trimers into the CM. Briefly, 7PA2 and untransfected Chinese hamster ovary (CHO) cell lines were grown to 95% confluency and conditioned in DMEM without serum for 16 h. Both CM as well as control CHO media was centrifuged (200g for 10 min) to remove debris and concentrated using a YM-3 column (Millipore) as described previously (Kurup et al. 2010). CM was aliquoted into 60 μl aliquots and stored at -20°C.

2.3 **Neuronal cultures**: Cortical cultures were grown from WT mice (postnatal day 0-2). For studying dendritic morphology and spine density, neuronal cultures were transfected with eGFP plasmid using DNA-CaCl2 method at day 3. Cultures were maintained for 18 days; after drug treatments, they were fixed with 4% paraformaldehyde. The cells were stained with anti-GFP and anti-MAP2 antibodies for analysis. Images were captured using Apotome at 20X (dendritic morphology analysis) and Leica confocal microscope 100X (spine density analysis). For dendritic morphology analysis, neuron tracing and subsequent Sholl analysis was done using Neurolucida software.

For synaptic puncta studies, neuronal cultures were grown for 18 days before addition of DMSO (0.1%) or TC-2153 at 1µM in the cell culture media for 48 hrs and was maintained during Aβ treatment. Cells were fixed using 4% paraformaldehyde for 10 min at room temperature. Cells were stained for the presynaptic marker, anti-synapsin (green) and the post synaptic marker, anti-PSD-95 (red). Images were captured using an Apotome microscope at 40X and analysis was performed using puncta analyzer software as described by (Ippolito and Eroglu 2010). Briefly, using the circular selection tool in the ImageJ menu to select a region radially around the soma of interest as region of interest (ROI). Both red and green channel images are thresholded and a rolling ball radius of 50 and minimum puncta size of 4 is selected. The results from the software provides quantification of red, green and colocalized puncta. Analysis was performed by researchers blinded to the experimental conditions.

Table 1: Materials used in the study

Cat No.	**Antibody/Drug**	**Company**
ab13552	PSD-95	Abcam
ab254349	Synapsin	Abcam
sc-9996	GFP	Santa cruz
sc-74421	MAP2	Santa cruz
SML1299	TC-2153	Sigma

For spine density analysis, spines were counted from dendrites with minimum 30um length. Using Image J line tool, the spines were manually traced by drawing a line from the base of the spine to the head. The total no of spines was divided by the total dendrite length to obtain density per um value.

2.4 Drug treatment and Golgi staining: WT and AD mice were treated with TC-2153 or vehicle (5% DMSO in saline) at a dose of 10mg/kg, i.p. for 14 days (Xu et al. 2014). Brains were perfused with 0.9% saline and incubated in Golgi-Cox (FD Neurotechnologies) impregnation solution for 14 days. Brains were then transferred to 30% sucrose for a week before slicing into 200µm thick sections. Sections were mounted on gelatin coated slides and stained as previously described (Milatovic et al. 2010). Images were captured using a Leica confocal microscope SP5 with 40X water immersion objective using the brightfield function and quantified by tracing using multipoint tool in ImageJ analysis software. Statistical analysis was done using GraphPad Prism software.

2.5 Statistical analysis

All data are represented as mean ± SEM. Data from each culture was averaged and then mean values from each cultures were plotted in the graph. Statistical differences were determined using two-way ANOVA with disease and drug treatment as variables using Graphpad Prism software. $P<0.05$ was considered significant. Researchers were blinded to the experimental condition.

3. Results

3.1 Aβ leads to loss of dendritic complexity in primary cortical neurons, which is rescued by STEP inhibition

We first examined the effects of exogenous application of conditioned media containing Aβ on dendritic complexity in neuronal cultures. We previously demonstrated that application of Aβ for 120 min. resulted in increased STEP levels in cortical neurons with concomitant tyrosine dephosphorylation of its substrates, including a reduction in GluN2B receptors on membrane fractions (Kurup et al. 2010). We therefore treated 18-day old cortical neurons with conditioned media from mutant CHO cells containing Aβ (7PA2-CM) and control media (CM) (Fig. 1). Neurons treated with 7PA2-CM showed significantly less dendritic complexity as analyzed by Sholl analysis. There was a significant decrease in the number of dendritic junctions or nodes ($P<0.01$) and ends ($P<0.05$) compared to CM treated neurons. Application of the STEP inhibitor, TC-2153 (1μM), has previously been shown to inhibit STEP activity in cortical cultures and restore the tyrosine phosphorylation of GluN2B receptor subunits (Tyr^{1472}) (Xu et al. 2014). We treated neurons with the inhibitor or vehicle for 48 hours prior to addition of either 7PA2-CM or CM. TC-2153 was maintained in culture and cells were fixed 24 hours after Aβ application and stained with MAP2 antibody. Again, we observed that neurons stimulated with 7PA2 (Fig 1C) showed significant reduction of dendritic complexity as compared with CM ($P<0.05$; Figure 1A). Pretreatment with TC-2153 to Aβ -treated cells significantly minimized the loss of dendritic complexity. In addition, TC-2153 pretreated Aβ cells had a greater number of nodes ($P<0.05$) and ends ($P<0.05$) compared to vehicle-treated Aβ cells (Figure 1A-G).

3.2 TC-2153 increases number of synaptic puncta in Aβ treated neurons

We next evaluated whether STEP inhibition prevented the loss of synapses in Aβ-treated neurons. We performed colocalization staining of the synaptic puncta using a pre-synaptic marker (synapsin) and a post-synaptic marker (PSD-95) and analyzed images using Puncta Analyzer (Ippolito and Eroglu 2010). Aβ-treated neurons showed significantly fewer colocalized synaptic puncta than CM-treated neurons ($P<0.05$) (Kono et al. 2019). Pre-treatment with TC-2153 significantly increased the colocalized synaptic puncta in Aβ-treated neurons ($P<0.001$) (Figure 2A-E).

3.3 TC-2153 attenuates spine loss in Aβ-treated neurons

Previous studies indicate that neurons exposed to Aβ show loss of spines (Calabrese et al. 2007; Shankar et al. 2007; Wei et al. 2010). Since Aβ contributes to the increase in STEP activity, we determined whether inhibition of STEP would contribute to spine loss as well. We treated transfected 3-day-old cortical neurons with pN1-EGFP and after 15 days, pretreated them with TC-2153 before adding Aβ. Consistent with previous studies, Aβ treatment resulted in a significant loss of dendritic spine density ($P<0.05$). However, TC-2153 pretreated cells showed no such loss of dendritic spine density ($P<0.05$, Figure 3E). These data indicate that TC-2153 inhibition of STEP prevents the Aβ–mediated loss of dendritic spine density.

3.4 TC-2153 treatment increases dendritic spine density in 3x Tg AD mice.

The increase in STEP levels in 3xTg mice is correlated with memory impairments (Kurup et al. 2010; Zhang et al. 2010). We previously showed that TC-2153 significantly rescued cognitive impairments in 6-month-old AD mice (Xu et al. 2014). To determine the effects of STEP inhibition on spine loss *in vivo*, we injected 6-month old 3xTg mice with TC-2153 (10 mg/kg, i.p.) for 14 days. Following treatment, their brains were Golgi stained and sectioned. Confocal analysis of cortical neurons showed a significant reduction of dendritic spine density in vehice-treated AD mice ($P<0.01$). Treatment with TC-2153 significantly rescued the dendritic spine density ($P<0.05$, Figure 4). These data suggest that inhibition of STEP might decrease the progression of neuronal deterioration in AD mice.

4. Discussion

STEP levels are elevated in Alzheimer's disease in both post-mortem human brain samples and mouse models of Alzheimer's disease (Kurup et al. 2010). We previously found that both genetic and pharmacological reduction of STEP activity rescued cognitive deficits in 3xTg mice (Zhang et al. 2010; Xu et al. 2014). Addtionally, STEP inhibition has been beneficial in maintaining synaptic homoeostasis in the hippocampal neurons in mouse models of fragile-X syndrome (Chatterjee et al. 2018). This is partly because activated STEP dephosphorylates NMDA and AMPA receptors and reduces their membrane expression. In this study, we provide evidence that cognitive improvements after STEP inhibition are accompanied by improvements in markers of healthy synaptic morphology, reinforcing the role of STEP in AD pathology.

STEP activity, Aβ levels, and synapse regulation are closely linked. Aβ is produced after proteolytic cleavage of amyloid precursor protein (APP). Studies have shown that Aβ oligomers reduce the density of spines in cultured neurons and transgenic mouse models (Lacor et al. 2004; Wei et al. 2010; Spires-Jones and Hyman 2014). Consistent with these structural abnormalities, neurons treated with Aβ or neurons that overexpress APP show depressed glutamatergic transmission (Ting et al. 2007). Exogenous application of Aβ induces endocytosis of NMDA receptors through a STEP-dependent pathway (Kurup et al. 2010). Since NMDA receptors are involved in the regulation of spine structure (Ultanir et al. 2007), STEP-mediated downregulation of NMDA recptors may contribute to the loss of synaptic density in AD.

Furthermore, recent studies report that F-actin (fibrillar actin) , a major cytoskeletal protein that determines the shape of spines, depolymerizes to G-actin (globular actin) upon Aβ exposure, thus contributing to the collapse and decrease of spines (Kommaddi et al. 2018). We believe that SPIN90, an additional substrate of STEP, facilitates in F-actin depolymerization (Kim et al. 2007). When SPIN90 is tyrosine phosphorylated, it binds to cofilin and reduces the actin-depolymerizing activity of cofilin (Cho et al. 2013a). When SPIN90 is dephosphorylated by STEP, it leads to cofilin activation and actin depolymerization, thereby contributing to spine shrinkage (Cho et al. 2013b). Phosphorylated SPIN90 also interacts with scaffolding proteins PSD95 and Shank in the postsynaptic compartment. It is well known that Shank promotes spine maturation and enlargement (Sala et al. 2001), and that PSD95 is involved in increasing spine density and the number of synapses (El-Husseini et al. 2000). Loss of synaptic clustering with

Shank and PSD95 after SPIN90 dephosphorylation by STEP affects both the size and density of dendritic spines (Cho et al. 2013a). Therefore, the inhibition of STEP using TC-2153 may prevent both the redistribution of SPIN90 in spines and possible malfunction of neural networks, resulting in improved cognition in AD mice.

5. Conclusion

As depicted in figure 5, our current model of AD pathophysiology suggests that Aβ inhibition of the ubiquitin degradation pathway results in increased levels of active STEP. Overactivation of STEP promotes internalization of NMDA and AMPA receptor complexes as well as dephosphorylation and translocation of SPIN90, causing spine loss after cofilin-mediated actin depolymerization. Inhibition of STEP using TC-2153 prevents this loss and rescues the pathologic synaptic morphology in conjunction with improved cognitive functioning. Long-term interventions studying TC-2153 treatment in 3xTg-AD mice, starting before the onset of memory symptoms and spine loss, may uncover the full therapeutic potential of STEP inhibitors.

Acknowledgments

We thank Ms, Clair Sulerzyski for technical assistance as well as laboratory members for helpful discussions. We are grateful to Tyler Baguley and Dr. Jonathan Ellmann of Yale Univeristy for providing TC-2153. MC and PL conceived of and designed the experiments. MC and PKK performed cell cultures and spine density studies. JK performed synaptic puncta experiments. MC, JK, JB and MK performed in vivo drug administration and Golgi staining experiments. MC and PL interpreted the data. MC, PKK and PL helped write the manuscript. All authors approved the final version of the submitted manuscript.

Funding

This work was supported by the National Institutes of Health grants MH091037 and MH52711 (P.J.L.), and a Swebilius Award and NARSAD grant (M.C.).

Declarations of interest

None.

References:

Calabrese B, Shaked GM, Tabarean IV, Braga J, Koo EH, Halpain S (2007) Rapid, concurrent alterations in pre- and postsynaptic structure induced by naturally-secreted amyloid-beta protein. Mol Cell Neurosci 35:183-193 doi: 10.1016/j.mcn.2007.02.006

Castonguay D, Dufort-Gervais J, Menard C, et al. (2018) The Tyrosine Phosphatase STEP Is Involved in Age-Related Memory Decline. Curr Biol 28:1079-1089 e1074 doi: 10.1016/j.cub.2018.02.047

Chatterjee M, Kurup PK, Lundbye CJ, et al. (2018) STEP inhibition reverses behavioral, electrophysiologic, and synaptic abnormalities in Fmr1 KO mice. Neuropharmacology 128:43-53 doi: 10.1016/j.neuropharm.2017.09.026

Chin J, Palop JJ, Puolivali J, et al. (2005) Fyn kinase induces synaptic and cognitive impairments in a transgenic mouse model of Alzheimer's disease. J Neurosci 25:9694-9703 doi: 10.1523/JNEUROSCI.2980-05.2005

Cho IH, Kim DH, Lee MJ, Bae J, Lee KH, Song WK (2013a) SPIN90 phosphorylation modulates spine structure and synaptic function. PLoS One 8:e54276 doi: 10.1371/journal.pone.0054276

Cho IH, Lee MJ, Kim DH, et al. (2013b) SPIN90 dephosphorylation is required for cofilin-mediated actin depolymerization in NMDA-stimulated hippocampal neurons. Cell Mol Life Sci 70:4369-4383 doi: 10.1007/s00018-013-1391-4

DeKosky ST, Scheff SW (1990) Synapse loss in frontal cortex biopsies in Alzheimer's disease: correlation with cognitive severity. Ann Neurol 27:457-464 doi: 10.1002/ana.410270502

El-Husseini AE, Schnell E, Chetkovich DM, Nicoll RA, Bredt DS (2000) PSD-95 involvement in maturation of excitatory synapses. Science 290:1364-1368

Ippolito DM, Eroglu C (2010) Quantifying synapses: an immunocytochemistry-based assay to quantify synapse number. J Vis Exp 45 doi: 10.3791/2270

Kashyap G, Bapat D, Das D, et al. (2019) Synapse loss and progress of Alzheimer's disease -A network model. Sci Rep 9:6555 doi: 10.1038/s41598-019-43076-y

Kim DJ, Kim SH, Kim SM, Bae JI, Ahnn J, Song WK (2007) F-actin binding region of SPIN90 C-terminus is essential for actin polymerization and lamellipodia formation. Cell Commun Adhes 14:33-43 doi: 10.1080/15419060701225010

Knobloch M, Mansuy IM (2008) Dendritic spine loss and synaptic alterations in Alzheimer's disease. Mol Neurobiol 37:73-82 doi: 10.1007/s12035-008-8018-z

Kommaddi RP, Das D, Karunakaran S, et al. (2018) Abeta mediates F-actin disassembly in dendritic spines leading to cognitive deficits in Alzheimer's disease. J Neurosci 38:1085-1099 doi: 10.1523/JNEUROSCI.2127-17.2017

Kono R, Kim GL, Nagata H, Ikegaya Y, Koyama R (2019) Induced neuronal activity does not attenuate amyloid beta-induced synaptic loss in vitro. Neuropsychopharmacol Rep 39:306-311 doi: 10.1002/npr2.12074

Kurup P, Zhang Y, Xu J, et al. (2010) Abeta-mediated NMDA receptor endocytosis in Alzheimer's disease involves ubiquitination of the tyrosine phosphatase STEP61. J Neurosci 30:5948-5957 doi: 10.1523/JNEUROSCI.0157-10.2010

Kurup PK, Xu J, Videira RA, Ononenyi C, Baltazar G, Lombroso PJ, Nairn AC (2015) STEP61 is a substrate of the E3 ligase parkin and is upregulated in Parkinson's disease. Proc Natl Acad Sci U S A 112:1202-1207 doi: 10.1073/pnas.1417423112

Lacor PN, Buniel MC, Chang L, et al. (2004) Synaptic targeting by Alzheimer's-related amyloid beta oligomers. J Neurosci 24:10191-10200 doi: 10.1523/JNEUROSCI.3432-04.2004

Li R, Xie DD, Dong JH, et al. (2014) Molecular mechanism of ERK dephosphorylation by striatal-enriched protein tyrosine phosphatase. J Neurochem 128:315-329 doi: 10.1111/jnc.12463

Milatovic D, Montine TJ, Zaja-Milatovic S, Madison JL, Bowman AB, Aschner M (2010) Morphometric analysis in neurodegenerative disorders. Curr Protoc Toxicol Chapter 12:Unit 12 16 doi: 10.1002/0471140856.tx1216s43

Ng AN, Doherty AJ, Lombroso PJ, Emptage NJ, Collingridge GL (2014) Rapid regulation of endoplasmic reticulum dynamics in dendritic spines by NMDA receptor activation. Mol Brain 7:60 doi: 10.1186/s13041-014-0060-3

Palop JJ, Mucke L (2010) Amyloid-beta-induced neuronal dysfunction in Alzheimer's disease: from synapses toward neural networks. Nat Neurosci 13:812-818 doi: 10.1038/nn.2583

Sala C, Piech V, Wilson NR, Passafaro M, Liu G, Sheng M (2001) Regulation of dendritic spine morphology and synaptic function by Shank and Homer. Neuron 31:115-130 doi: 10.1016/s0896-6273(01)00339-7

Scheff SW, Price DA, Schmitt FA, Mufson EJ (2006) Hippocampal synaptic loss in early Alzheimer's disease and mild cognitive impairment. Neurobiol Aging 27:1372-1384 doi: 10.1016/j.neurobiolaging.2005.09.012

Shankar GM, Bloodgood BL, Townsend M, Walsh DM, Selkoe DJ, Sabatini BL (2007) Natural oligomers of the Alzheimer amyloid-beta protein induce reversible synapse loss by modulating an NMDA-type glutamate receptor-dependent signaling pathway. J Neurosci 27:2866-2875 doi: 10.1523/JNEUROSCI.4970-06.2007

Snyder EM, Nong Y, Almeida CG, et al. (2005) Regulation of NMDA receptor trafficking by amyloid-beta. Nat Neurosci 8:1051-1058 doi: 10.1038/nn1503

Spires-Jones TL, Hyman BT (2014) The intersection of amyloid beta and tau at synapses in Alzheimer's disease. Neuron 82:756-771 doi: 10.1016/j.neuron.2014.05.004

Terry RD, Masliah E, Salmon DP, et al. (1991) Physical basis of cognitive alterations in Alzheimer's disease: synapse loss is the major correlate of cognitive impairment. Ann Neurol 30:572-580 doi: 10.1002/ana.410300410

Ting JT, Kelley BG, Lambert TJ, Cook DG, Sullivan JM (2007) Amyloid precursor protein overexpression depresses excitatory transmission through both presynaptic and postsynaptic mechanisms. Proc Natl Acad Sci U S A 104:353-358 doi: 10.1073/pnas.0608807104

Ultanir SK, Kim JE, Hall BJ, Deerinck T, Ellisman M, Ghosh A (2007) Regulation of spine morphology and spine density by NMDA receptor signaling in vivo. Proc Natl Acad Sci U S A 104:19553-19558 doi: 10.1073/pnas.0704031104

Venkitaramani DV, Paul S, Zhang Y, et al. (2009) Knockout of striatal enriched protein tyrosine phosphatase in mice results in increased ERK1/2 phosphorylation. Synapse 63:69-81 doi: 10.1002/syn.20608

Walsh DM, Klyubin I, Fadeeva JV, et al. (2002) Naturally secreted oligomers of amyloid beta protein potently inhibit hippocampal long-term potentiation in vivo. Nature 416:535-539 doi: 10.1038/416535a

Wei W, Nguyen LN, Kessels HW, Hagiwara H, Sisodia S, Malinow R (2010) Amyloid beta from axons and dendrites reduces local spine number and plasticity. Nat Neurosci 13:190-196 doi: 10.1038/nn.2476

Wu PH, Coultrap SJ, Browning MD, Proctor WR (2011) Functional adaptation of the N-methyl-D-aspartate receptor to inhibition by ethanol is modulated by striatal-enriched protein tyrosine phosphatase and p38 mitogen-activated protein kinase. Mol Pharmacol 80:529-537 doi: 10.1124/mol.110.068643

Xu J, Chatterjee M, Baguley TD, et al. (2014) Inhibitor of the tyrosine phosphatase STEP reverses cognitive deficits in a mouse model of Alzheimer's disease. PLoS Biol 12:e1001923 doi: 10.1371/journal.pbio.1001923

Xu J, Hartley BJ, Kurup P, et al. (2018) Inhibition of STEP61 ameliorates deficits in mouse and hiPSC-based schizophrenia models. Mol Psychiatry 23:271-281 doi: 10.1038/mp.2016.163

Xu J, Kurup P, Bartos JA, Patriarchi T, Hell JW, Lombroso PJ (2012) Striatal-enriched protein-tyrosine phosphatase (STEP) regulates Pyk2 kinase activity. J Biol Chem 287:20942-20956 doi: 10.1074/jbc.M112.368654

Zhang L, Xie JW, Yang J, Cao YP (2013) Tyrosine phosphatase STEP61 negatively regulates amyloid beta-mediated ERK/CREB signaling pathways via alpha7 nicotinic acetylcholine receptors. J Neurosci Res 91:1581-1590 doi: 10.1002/jnr.23263

Zhang Y, Kurup P, Xu J, et al. (2010) Genetic reduction of striatal-enriched tyrosine phosphatase (STEP) reverses cognitive and cellular deficits in an Alzheimer's disease mouse model. Proc Natl Acad Sci U S A 107:19014-19019 doi: 10.1073/pnas.1013543107

Zhang Y, Venkitaramani DV, Gladding CM, et al. (2008) The tyrosine phosphatase STEP mediates AMPA receptor endocytosis after metabotropic glutamate receptor stimulation. J Neurosci 28:10561-10566 doi: 10.1523/JNEUROSCI.2666-08.2008

Figure legends:

Figure 1: STEP inhibition prevents the loss of dendritic complexity in Aβ-treated primary cortical neurons. Primary cortical cultures (DIV-18) were treated with Vehicle (0.1% DMSO) or TC-2153 48hrs prior to addition of CHO media or conditioned media containing Aβ and immunostained with MAP2 antibody. Representative images and their respective Sholl graphs of primary cortical neuron from CHO + Veh (A); CHO+TC (B) Aβ+Veh (C) and Aβ+TC (D). Quantification of number of intersections from the soma (E). Quantification and analysis of numbers of Nodes (F) and Ends (G) across various groups. (Data from 5 neurons per culture per condition, 3-4 cultures; ***P<0.001; *P<0.05; 2-way ANOVA, Tukey post hoc analysis)

Figure 2: TC-2153 treatment rescues the loss of synaptic puncta in Aβ-treated neurons. WT cortical cultures were treated with TC-2153 or vehicle at DIV18, prior to addition of CHO media or conditioned media containing Aβ. Cells were stained with anti-synapsin (green) and anti-PSD-95 (red). Representative images of (A) CHO+Veh (B) CHO+TC (C) Aβ+Veh (D) Aβ+TC. Quantifications of number of colocalized puncta across all groups (E). The scale bar represents 10μm (n = 20 synapses per condition per culture, 3-4 cultures; ***P<0.001; *P<0.05; 2-way ANOVA, Tukey post hoc analysis)

Figure 3: TC-2153 rescues the loss of spines in Aβ treated neurons. WT cortical cultures were transfected with eGFP on DIV-3 and treated with TC-2153 or vehicle at DIV18, prior to addition of CHO media or conditioned media containing Aβ. Cells were fixed with 4% PFA and stained with anti-GFP antibody. Representative confocal images show Representative images of (A) CHO+Veh (B) CHO+TC (C) Aβ+Veh (D) Aβ+TC are shown. Quantifications of spine density across all groups (E). Data represents Mean + SEM. (n= 5 neurons per culture per condition, 3-4 cultures; *P<0.05; 2-way ANOVA, Tukey post hoc analysis)

Figure 4: TC-2153 rescues the loss of spines in 3xTg mice. WT and 3xTg-AD mice (6-month old) were treated with TC-2153 or vehicle for 14 days. The animals were sacrificed, and the

brains were collected and subjected to Golgi staining. Representative confocal images of Golgi stained sections of WT+Veh (A) WT+ TC (B) AD +Veh (C) and AD+TC (D) ;showing reduction in spine density in AD mice (C) in comparison to WT mice (A). The spine loss shows a significant improvement in mice treated with TC-2153 (E). (10 neurons per mice, n = 6 mice per group, *$P < 0.05$, 2-way ANOVA, Tukey post hoc analysis).

Figure 5: Diagrammatic representation of the current model. Aβ binding to α7nAChRs and synaptic NMDAR stimulation invokes activation of PP2B/calcineurin and PP1 to dephosphorylate STEP61, thereby increasing the affinity of STEP61 for its substrates. In a parallel pathway, Aβ inhibits the ubiquitin proteasome system (UPS) and prevents degradation of STEP61. The net result is an accumulation of active STEP protein levels in AD, which leads to increased dephosphorylation and internalization of GluN2B-containing NMDARs as well as dephosphorylation and translocation of SPIN90 to dendritic shaft. This causes release of its binding partner cofilin which severs F-actin to G-actin and thereby causes spine loss.

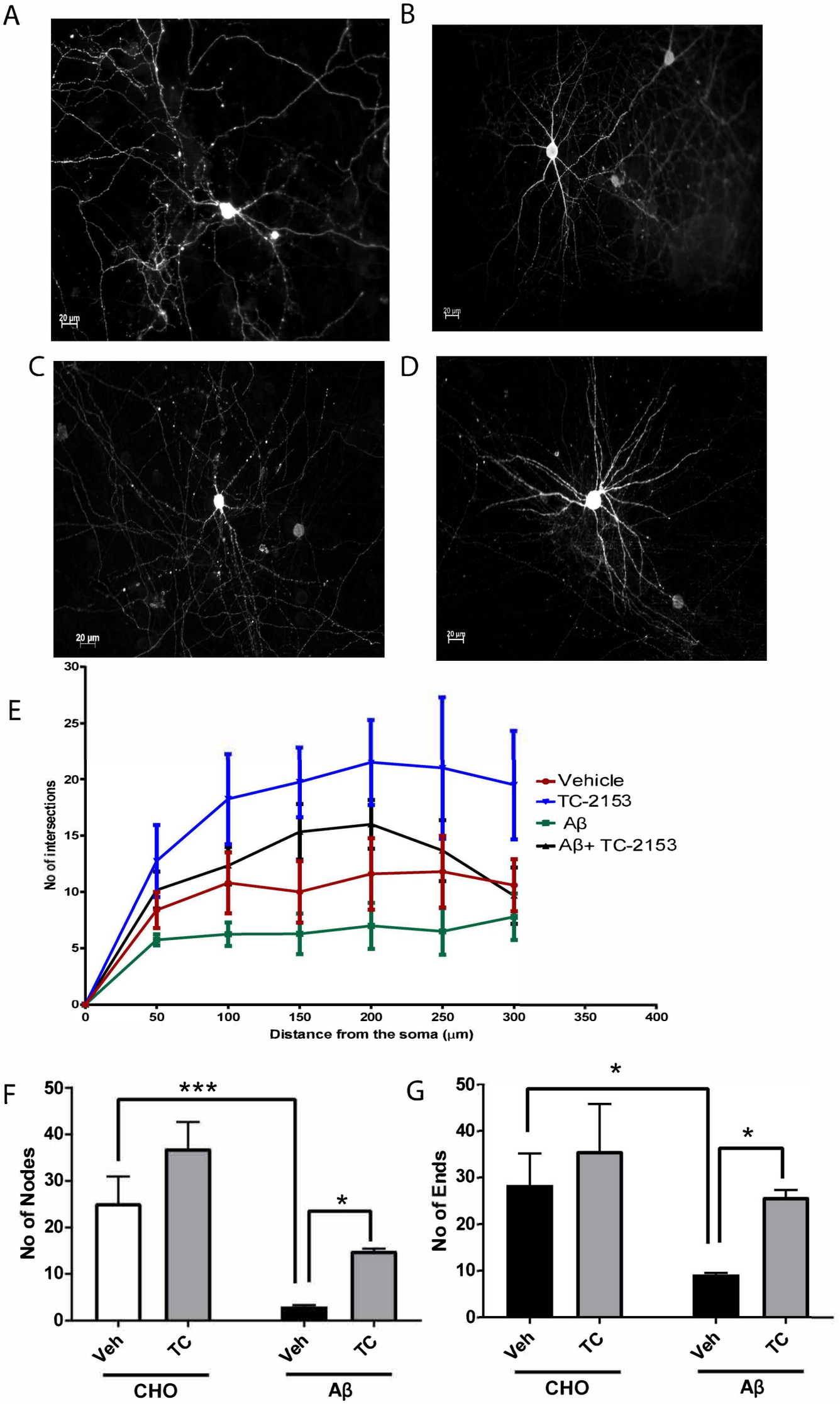
A
B
C
D
20 µm
E
No of intersections
Distance from the soma (µm)
Vehicle
TC-2153
Aβ
Aβ+ TC-2153
F
No of Nodes
***
*
Veh
TC
CHO
Aβ
G
No of Ends
*
*

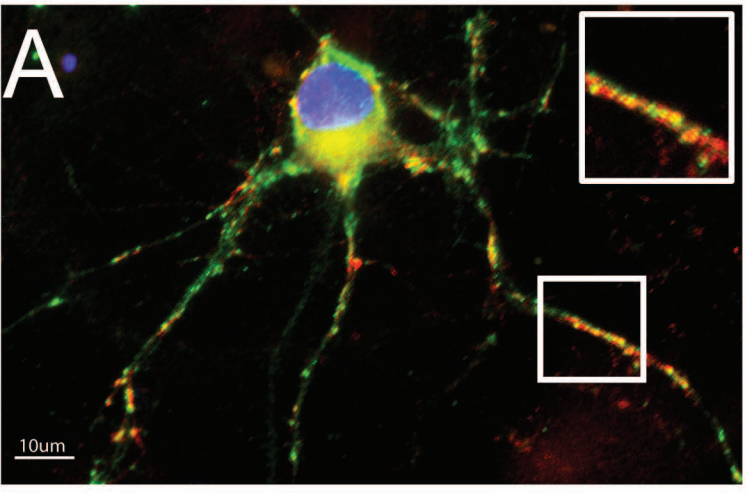
A
10um

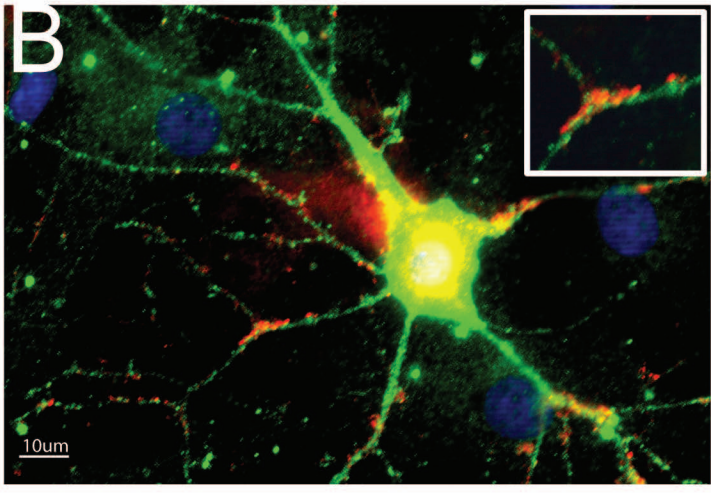
B
10um

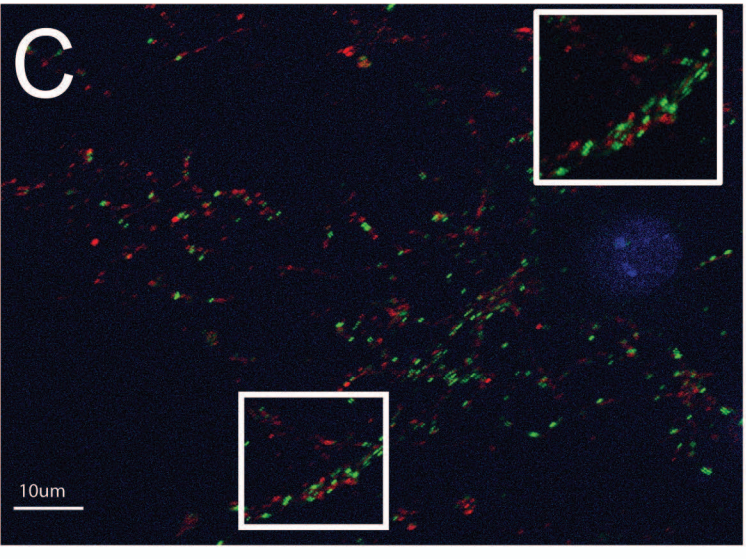
C
10um

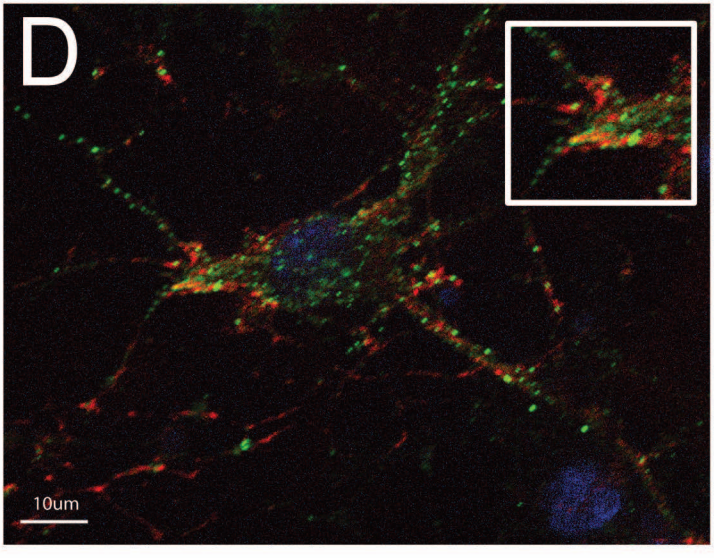
D
10um

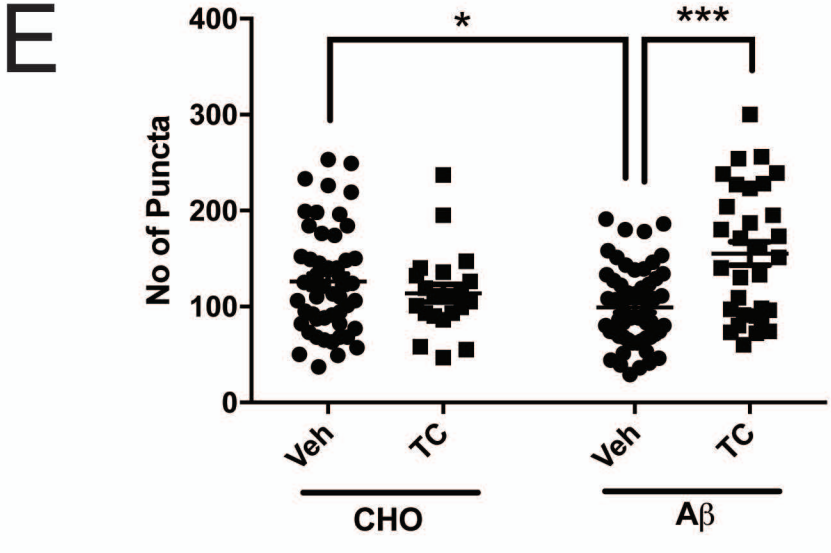
E
No of Puncta
400
300
200
100
0
*
***
Veh
TC
Veh
TC
CHO
Aβ

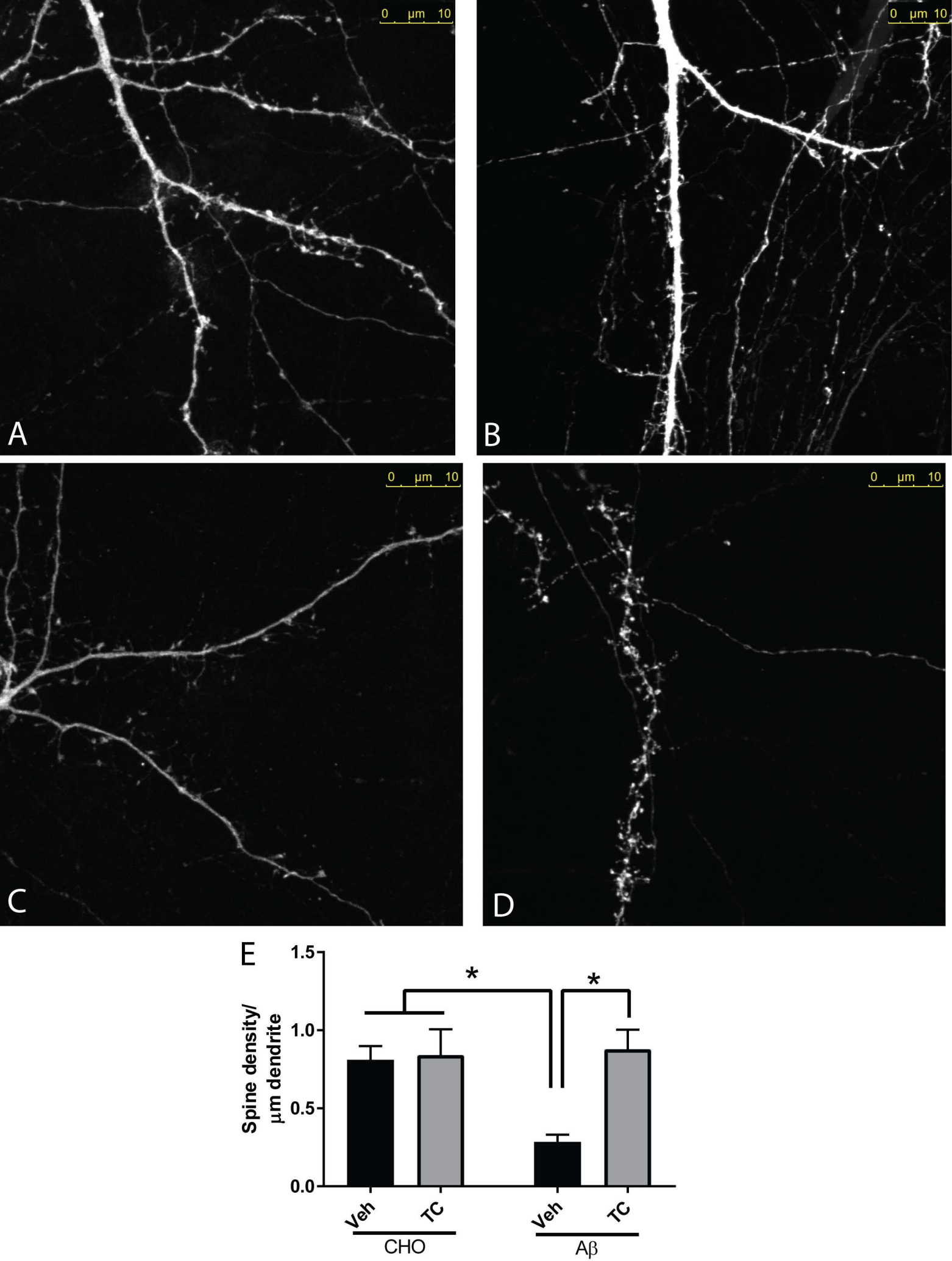
0 µm 10
A
B
C
D
E
Spine density/
µm dendrite
1.5
1.0
0.5
0.0
*
*
Veh
TC
Veh
TC
CHO
Aβ

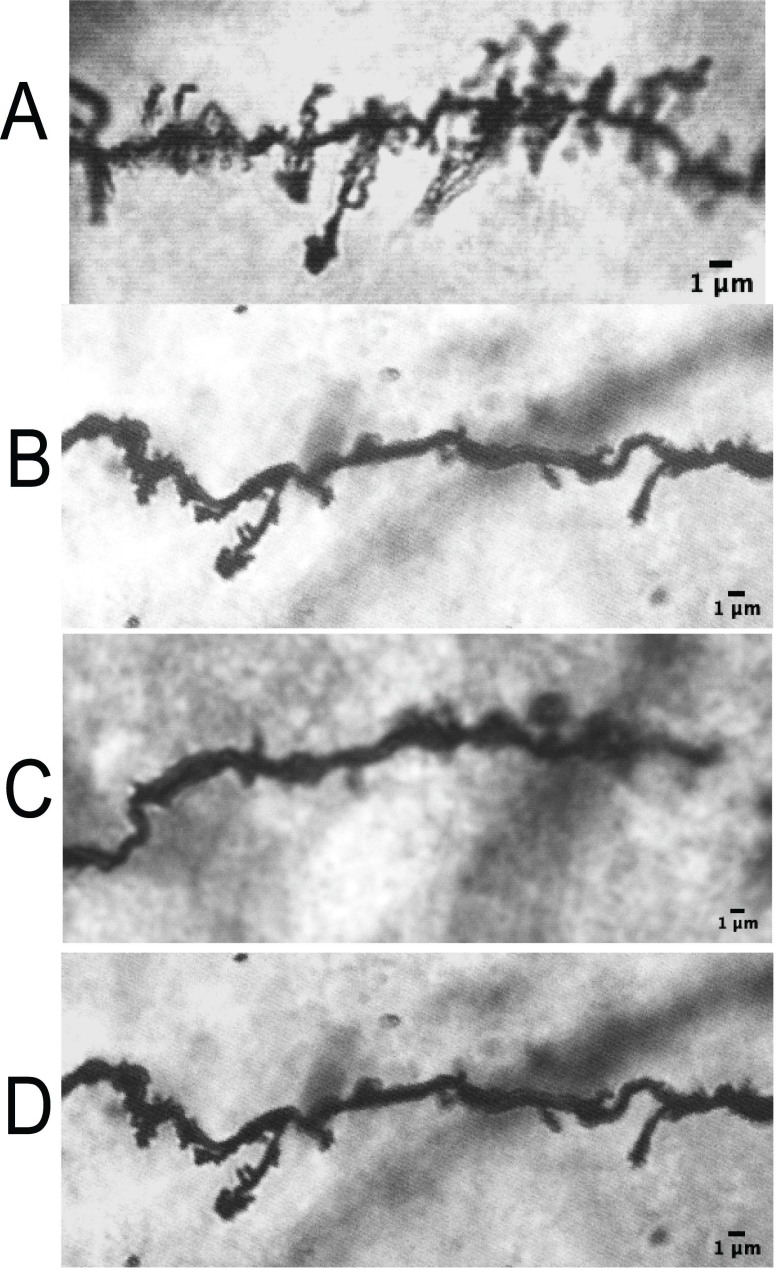
A
1 µm
B
1 µm
C
1 µm
D
1 µm

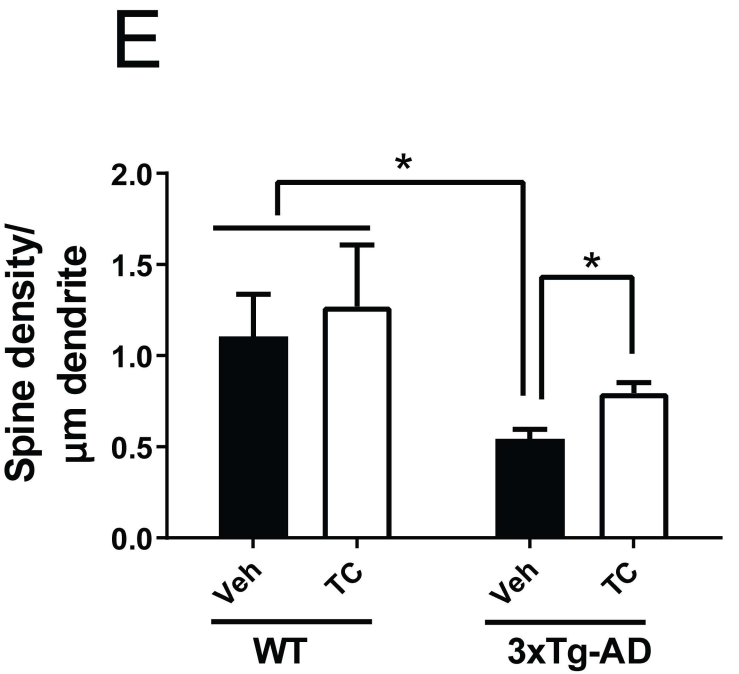
E
Spine density/
µm dendrite
2.0
1.5
1.0
0.5
0.0
*
*
Veh
TC
Veh
TC
WT
3xTg-AD

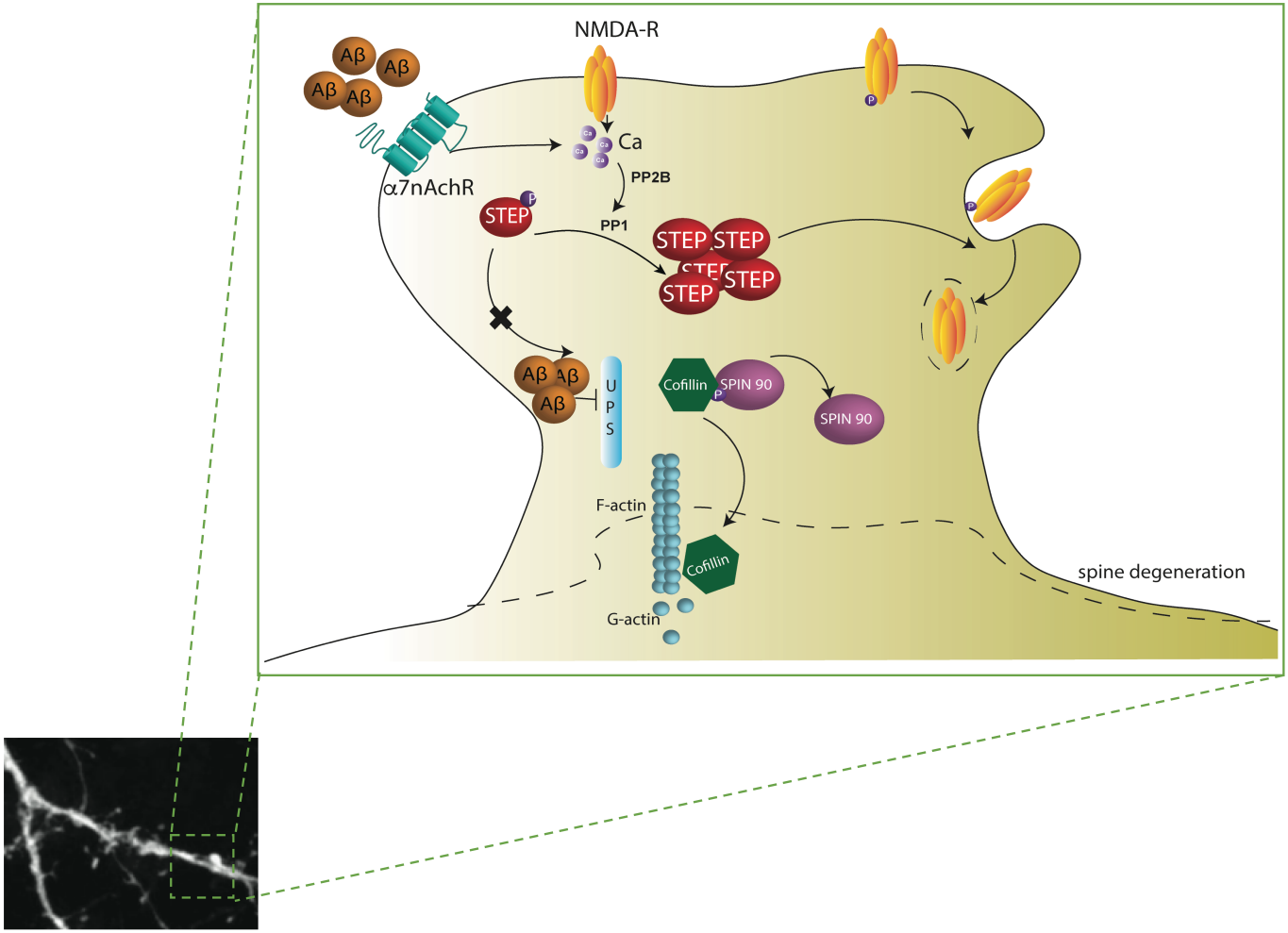
NMDA-R
Aβ
Aβ
Aβ
Aβ
α7nAchR
Ca
PP2B
PP1
STEP
P
STEP
STEP
STEP
STEP
STEP
Aβ
Aβ
Aβ
U
P
S
Cofillin
SPIN 90
P
SPIN 90
F-actin
Cofillin
G-actin
spine degeneration